Progress In Electromagnetics Research B, Vol. 57, 87–104, 2014

Large-signal Field Analysis of a Linear Beam Traveling Wave Amplifier for a Sheath-helix Model of the Slow-wave Structure Supported by Dielectric Rods. Part 1: Theory

Natarajan Kalyanasundaram* and Amita Agnihotri

Abstract—A rigorous field-theoretic method of analyzing the large-signal behavior of a linear beam traveling wave tube amplifier (TWTA) with slow-wave structure modeled to be a dielectric-loaded sheath helix is presented. The key step in the analysis is a representation of the field components as nonlinear functionals of the electron arrival time through a Green's function sequence for the slow-wave circuit. Substitution of this functional representation for the axial electric field component into the electron ballistic equation casts the latter into a fixed point format for a nonlinear operator in an appropriate function space. The fixed point, and therefore the solution for the electron-arrival time and hence the solution for the electromagnetic field components, can be obtained by standard successive approximation techniques. The calculations of the gain, the efficiency and the other amplifier parameters, comparison of the results of the present theory with experimental results etc., on the basis of such a successive approximation solution for the field components, will be presented in the second part of this paper.

1. INTRODUCTION

Ever since the invention by Rudolf Kompfner in 1943, the linear beam traveling wave tubes making use of an helix for the slow-wave structure (popularly known as helix TWTs), with their wide bandwidths and large power outputs, continue to be unsurpassed as broadband amplifiers of microwave power except possibly by gyro-TWTs. The phenomenal growth of the satellite communication industry and the proliferation of radar applications have fueled an unprecedented demand for TWTs meeting stringent design specifications. In high power applications, the traveling wave tube amplifier (TWTA) will invariably be operated on the verge of saturation, and hence an analytical study of its large-signal behavior will be of immense interest.

The analysis of TWT as an amplifier has been carried out by Pierce and Kompfner [1–3]. This theory was developed some six and half decades ago, and it was based on a coupled-wave analysis utilizing the vacuum modes of the helix and the positive and the negative energy space — charge waves of the beam. An improved theory based on an eigen-vector analysis of Maxwell's equations for the helix has been developed by Reydbeck [4]. Chu and Jackson [5] and Collin [6] considered the field approach for a small-signal analysis of the helix-TWTA. The linearized 'solution' [6] for the axial electric field was obtained as a linear combination of three space charge waves, a growing wave and a decaying wave, both having phase speeds slightly smaller than the beam speed and a constant-amplitude wave with a phase speed greater than the beam speed. However, the input boundary conditions (that the total a.c. beam current density and the r.f. perturbation in the electron speed vanish at the input plane) could exactly be satisfied for a finite beam only by the trivial solution as the (complex) phase-shift constants associated with the three waves were not equal. Moreover, in the nonlinear regime this approach is completely intractable without the introduction of multitudinous limiting assumptions [7]. Freund et al. [8, 9] presented a linear field analysis for a TWTA using radial admittances at the boundaries. The analyses

Received 11 September 2013, Accepted 24 November 2013, Scheduled 30 November 2013
* Corresponding author: Natarajan Kalyanasundaram (n.kalyanasundaram@jiit.ac.in).
The authors are with the Jaypee Institute of Information Technology, A-10, Sector-62, Noida-201307, Uttar Pradesh, India.

were based on the coupled-mode theory [8] and the linearized relativistic field theory [9]. Being linear theories, they are not applicable to large signals.

The results of many attempts at developing a large-signal theory for the linear beam TWTA have been summarized in [7] and Detweiler and Rowe [10]. However, all of these studies make use of a transmission-line analogy to what is essentially a field problem, and suffer from at least the following two serious drawbacks:

1. The slow wave structure is modeled by a linear transmission-line circuit that is equivalent to it only in the small-signal limit, and this only at a single frequency, for the study of large-signal electron-wave interaction phenomena.
2. The electron stream entering the interaction region is arbitrarily divided into a finite number of discrete charge groups, and in the subsequent motion each charge group is treated as a single entity with complete disregard for the relative motion of the electrons within.

It is a well-known fact that when the TWTA is operated under large input-signal conditions, crossing of electron trajectories invariably takes place because of which the electron speed ceases to be single-valued when expressed as a function of the usual Eulerian spatial coordinates. Hence, recourse has to be made in the nonlinear case to the Lagrangian description wherein the entering electrons are indexed by their respective entrance times and the radial and the angular positions at the entrance plane, thereby obviating the need to have to deal with a multi-valued function. A rigorous field-theory based method of analyzing the large-signal behavior of a TWTA for an open sheath-helix model for the slow wave structure was presented for the first time by Kalyanasundaram [11] and Kalyanasundaram and Chinnadurai [12, 13] resorting to such a Lagrangian description for the electron trajectories.

In this paper, the large-signal field analysis method of [11] is extended to the practically relevant model of a sheath-helix supported inside a coaxial perfectly cylindrical shell by symmetrically disposed wedge-shaped dielectric rods (Fig. 1(a)). In order to make the analysis of the TWTA tractable, the above model of the slow-wave structure is simplified further by replacing the azimuthally periodic dielectric constant of the tubular region between the helix and the outer conductor by its azimuthally averaged constant value ε_{eff} (Fig. 1(b)). The azimuthally periodic nonhomogeneous relative permittivity $\varepsilon(\bar{r}, \varphi)$ of the tubular region between the sheath helix and the outer conductor for L symmetrically disposed wedge-type support rods of angular width $2\pi\sigma/L$ and dielectric constant ε_r is given by

$$\begin{aligned}\varepsilon(\bar{r},\varphi) &= \varepsilon_r \quad \text{for} \quad \pi(2l-\sigma)/L \le \varphi \le \pi(2l+\sigma)/L \\ &= 1 \quad \text{for} \quad \pi(2l+\sigma)/L \le \varphi \le \pi((2l+2)-\sigma)/L \\ &\qquad\quad \text{for} \quad \bar{a} \le \bar{r} \le \bar{b} \quad \text{and} \quad l = 0, 1, 2, \ldots, L-1.\end{aligned}$$

where $\bar{r}$, $\bar{a}$ and $\bar{b}$ are the radial coordinate, helix radius and outer-conductor radius, respectively (see the next section). Therefore, the effective dielectric constant of the medium between the sheath helix

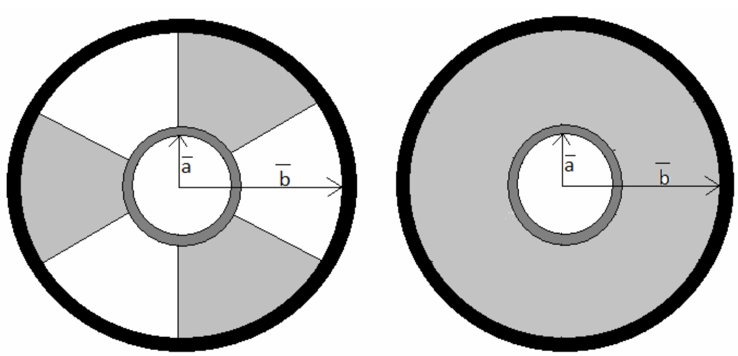

(a) (b)

Figure 1. Cross-sectional view of a dielectric-loaded sheath helix model: (a) Actual structure with three support rods of dielectric constant ε_r. (b) Azimuthally averaged structure with an effective dielectric constant $\varepsilon_{eff} = (1-\sigma) + \sigma\varepsilon_r$ for the region between the sheath helix and the outer conductor.

and the outer conductor works out to be

$$\varepsilon_{\mathit{eff}} \triangleq \frac{1}{2\pi}\int_0^{2\pi} \varepsilon(\bar{r},\varphi)d\varphi = (1-\sigma) + \sigma\varepsilon_r$$

where the symbol '$\triangleq$' denotes equality by definition. This simplified model of the slow-wave structure will be referred to as 'dielectric-loaded sheath helix' in the sequel. When the cross-sectional shape of the symmetrically loaded dielectric support rods is anything other than a wedge $\{(\bar{r},\varphi)\colon \bar{a} \le \bar{r} \le \bar{b}, \varphi_1 \le \varphi \le \varphi_2\}$ of angular width $\varphi_2 - \varphi_1$, the azimuthally averaged value of the dielectric constant will turn out to be a function of the radial coordinate: $\varepsilon_{\mathit{eff}}(\bar{r})$, $\bar{a} \le \bar{r} \le \bar{b}$. In this case, the region between the sheath helix and the outer conductor is partitioned into a finite number of tubular layers and each layer is characterized by the radially-averaged (constant) value of $\varepsilon_{\mathit{eff}}(\bar{r})$ over its radial thickness. This is equivalent to approximating $\varepsilon_{\mathit{eff}}(\bar{r})$ by a piecewise constant function in the radial variable $\bar{r}$. The solution for the field components over the entire region between the sheath helix and the outer conductor can then be recovered from the solutions for all the layers with constant values for the effective dielectric constant by enforcing the continuity of the tangential field components across the interfaces separating two adjacent tubular layers with different values for the effective dielectric constant. A similar approach has been adopted by Jain and Basu [14] to derive the dispersion relation governing the guided propagation of cold electromagnetic waves through a tape helix supported by dielectric rods of circular cross section on the basis of an ad hoc assumption about the tape-current distribution.

As in [11], the axial electric field component inside the electron beam is represented, invoking the steady-state assumption, as a nonlinear functional of the electron-arrival time through a sequence of Green's functions for the slow-wave structure which is a dielectric-loaded sheath helix in the present case. Substitution of the resulting expression for this field component into electron ballistic equation casts the latter into a fixed point format for an operator in an appropriate function space. The fixed point, and hence the solution for the electron-arrival time can then be obtained by standard successive approximation techniques, the convergence of the sequence of successive approximations being guaranteed by the classical Banach fixed point theorem. Once we have the solution for the electron-arrival time, the expressions for the electromagnetic field components readily follow. The numerical computations of the gain, the efficiency and the other amplifier parameters, comparison of the theoretical predictions with the available experimental results etc., will be deferred to the second part of this paper.

2. PROBLEM FORMULATION

In this paper, only a steady-state solution corresponding to a single-frequency input excitation will be sought. Moreover, the following assumptions regarding the slow-wave circuit and the electron beam will be made use of in the formulation and the subsequent field analysis of the nonlinear electron-wave interaction phenomenon:

(i) Dielectric-loaded sheath-helix model for the slow-wave circuit.
(ii) Axially symmetric mode of operation.
(iii) Axially confined electron beam partially filling the tube.
(iv) Nonrelativistic operation justifying the dropping of r.f. magnetic force terms from the electron ballistic equation.
(v) Transverse electric field has negligible effect on the electron motion.
(vi) Electrons enter the interaction region with zero transverse speed.
(vii) The axial speed v_0 and the charge density ρ_0 of the entering electron stream remain constants with respect to the transverse co-ordinates and the time.
(viii) The electron entrance speed v_0 is assumed to be close to the cold-wave phase speed v_p at the input signal frequency $\omega_0/2\pi$ in order to meet the condition of approximate synchronism between the electron beam and the traveling electromagnetic wave.

Since it is desirable to carry out the analysis of the problem to be formulated in this section in terms of dimensionless variables, all dimensional variables will be distinguished from their dimensionless counterparts with an over bar in the notation for the dimensional variables. Accordingly, the axis of the tube (helix) is taken along the $\bar{z}$-co-ordinate of a cylindrical polar co-ordinate system ($\bar{r}$, φ, $\bar{z}$). The electron stream is assumed to enter the interaction region at the plane $\bar{z} = 0$. In addition to rendering the dependent and the independent variables dimensionless, the beam radius $\bar{a}_0$, the helix radius $\bar{a}$ and the inner radius $\bar{b}$ of the outer conductor are rendered dimensionless by dividing by the helix radius to yield the corresponding dimensionless versions $a = \bar{a}_0/\bar{a}$, $1 = \bar{a}/\bar{a}$ and $b = \bar{b}/\bar{a}$ respectively. The interaction length $\bar{d}$ of the tube is, however, rendered dimensionless according to $d = \omega_0\bar{d}/v_0$, where ω_0 is the angular frequency of the r.f. input signal and v_0 is the mean value of the axial electron speed at the entrance plane $\bar{z} = 0$. Notations for the various independent and dependent variables together with an explanation of the notation are given in Table 1(a) and Table 1(b) respectively.

In Table 1(b), Z_0 is the intrinsic impedance of free space and $A_0 (\triangleq \sup_t |\bar{\mathcal{E}}_1(0, \bar{a}, \bar{t})|)$ is the amplitude of axial electric field component at $\bar{z} = 0$, $\bar{r} = \bar{a}$.

From Table 1(b), and the definition of the axial electron speed (assumed to be always positive), we have

$$v(z, r, t_0) = 1/t_z(z, r, t_0) \tag{1}$$

Table 1. (a) Notation and terminology for independent variables. (b) Notation and terminology for dependent variables.

(a)

Dimensional Variables	Dimensionless Variables
$\bar{z}$ axial co-ordinate	$z = \omega_0\bar{z}/v_0$
$\bar{r}$ radial co-ordinate	$r = \bar{r}/\bar{a}$
$\bar{t}$ time	$t = \omega_0\bar{t}$
$\bar{t}_0$ electron entrance time	$t_0 = \omega_0\bar{t}_0$

(b)

Dimensional Variables	Dimensionless Variables
$\bar{t}(\bar{z},\bar{r},\bar{t}_0)$: time of arrival at the location $(\bar{z},\bar{r})$ of an electron with entrance time $\bar{t}_0$	$t(z, r, t_0) = \omega_0\bar{t}(\bar{z},\bar{r},\bar{t}_0)$
$\bar{v}(\bar{z},\bar{r},\bar{t}_0)$: axial speed at the location $(\bar{z},\bar{r})$ of an electron with entrance time $\bar{t}_0$	$v(z, r, t_0) = \bar{v}(\bar{z},\bar{r},\bar{t}_0) / v_0$
$\bar{\rho}(\bar{z},\bar{r},\bar{t}_0)$: electron charge density	$\rho(z, r, t) = v_0^2 Z_0 \bar{\rho}(\bar{z},\bar{r},\bar{t}_0) / \omega_0 A_0$
$\bar{i}(\bar{z},\bar{r},\bar{t}_0)$: convection current density	$i(z, r, t) = v_0 Z_0 \bar{i}(\bar{z},\bar{r},\bar{t}_0) / \omega_0 A_0$
$\bar{\mathcal{E}}_k(\bar{z},\bar{r},\bar{t})$: for $k = 1,2,3$, axial, azimuthal and radial component of electric field vector	$\mathcal{E}_k(z, r, t) = \bar{\mathcal{E}}_k(\bar{z},\bar{r},\bar{t})/A_0$ for $k=1,2,3$
$\bar{\mathcal{H}}_k(\bar{z},\bar{r},\bar{t})$: for $k = 1,2,3$, axial, azimuthal and radial component of magnetic field vector	$\mathcal{H}_k(z, r, t) = Z_0\bar{\mathcal{H}}_k(\bar{z},\bar{r},\bar{t})/A_0$ for $k=1,2,3$

In (1) and in the following, an independent-variable subscript denotes partial differentiation with respect to that variable. From the law of conservation of charge [15], we obtain

$$i(z,r,t) = \sum_l q_0/|t_{t_0}(z,r,t_{0l}(z,r,t))| \tag{2a}$$

and hence using (1), we have

$$\rho(z,r,t) = \sum_l q_0 t_z(z,r,t_{0l}(z,r,t))/|t_{t_0}(z,r,t_{0l}(z,r,t))| \tag{2b}$$

where $q_0(\triangleq v_0^2\rho_0 Z_0/\omega_0 A_0)$ is both the dimensionless beam current density and the charge density at the entrance plane and the summation in (2) is over all roots (a finite number depending on the values of z, r and t) of the equation

$$t(z,r,t_0) = t$$

for t_0. The lth term in the summation on the right sides of (2a) and (2b) denotes respectively the contribution to the convection current density $i(z,\, r,\, t)$ and the charge density $\rho(z,\, r,\, t)$ from an electron with entrance time $t_{0l}(z,\, r,\, t)$. Thus the convection current density $i(z,\, r,\, t)$ and charge density $\rho(z,\, r,\, t)$ have contributions from all those electrons arriving at the location $(z,\, r)$ at time t irrespective of the order of their arrivals. The absolute value sign on t_{t_0} in (2) corresponds physically to the fact that the contributions to the charge and the current densities have the same sign irrespective of the order in which the contributing electrons arrive at the location $(z,\, r)$ [15].

Making use of the definitions of the dimensionless variables and parameters and invoking the simplifying assumptions from the beginning of this section, Maxwell's field equations and the electron ballistic equation can be expressed in dimensionless form as

$$a_1\kappa(r)\boldsymbol{\mathcal{E}}_{1_t} - a_2\left(\boldsymbol{\mathcal{H}}_{2_r} + \boldsymbol{\mathcal{H}}_2/r\right) = -i(z,r,t) = -q_0\sum_l |t_{t_0}(z,r,t_{0l}(z,r,t))|^{-1} \tag{3a}$$

$$a_1\kappa(r)\boldsymbol{\mathcal{E}}_{2_t} - \boldsymbol{\mathcal{H}}_{3_z} + a_2\boldsymbol{\mathcal{H}}_{1_r} = 0 \tag{3b}$$

$$a_1\kappa(r)\boldsymbol{\mathcal{E}}_{3_t} + \boldsymbol{\mathcal{H}}_{2_z} = 0 \tag{3c}$$

$$a_1\boldsymbol{\mathcal{H}}_{1_t} + a_2\left(\boldsymbol{\mathcal{E}}_{2_r} + \boldsymbol{\mathcal{E}}_2/r\right) = 0 \tag{4a}$$

$$a_1\boldsymbol{\mathcal{H}}_{2_t} + \boldsymbol{\mathcal{E}}_{3_z} - a_2\boldsymbol{\mathcal{E}}_{1_r} = 0 \tag{4b}$$

$$a_1\boldsymbol{\mathcal{H}}_{3_t} - \boldsymbol{\mathcal{E}}_{2_z} = 0 \tag{4c}$$

$$\boldsymbol{\mathcal{E}}_{1_z} + a_2\left(\boldsymbol{\mathcal{E}}_{3_r} + \boldsymbol{\mathcal{E}}_3/r\right) = \rho(z,r,t)/a_1 = \sum_l q_0 t_z(z,r,t_{0l}(z,r,t))/\left|t_{t_0}(z,r,t_{0l}(z,r,t))\right| \tag{5}$$

$$\boldsymbol{\mathcal{H}}_{1_z} + a_2\left(\boldsymbol{\mathcal{H}}_{3_r} + \boldsymbol{\mathcal{H}}_3/r\right) = 0 \tag{6}$$

$$t_{zz}(z,r,t_0) = \varepsilon(t_z(z,r,t_0))^3\boldsymbol{\mathcal{E}}_1(z,r,t(z,r,t_0)) \tag{7}$$

where the piecewise constant function $\kappa(r)$ is defined as

$$\kappa(r) = \begin{cases} 1 & \text{if} \quad 0 \le r < 1 \\ \varepsilon_{\mathit{eff}} & \text{if} \quad 1 < r < b \end{cases}$$

and $a_1 = v_0/c$, $a_2 = (v_0/\omega_0\bar{a})$, $\varepsilon = A_0 e/m_e\omega_0 v_0$ and where e/m_e is the charge magnitude-to-rest mass ratio of an electron. The dimensionless parameter ε is a measure of the input excitation. Equations (3)–(7) constitute an highly nonlinear coupled system of differential equations for the seven scalar functions $\boldsymbol{\mathcal{E}}_k(z,\, r,\, t)$ and $\boldsymbol{\mathcal{H}}_k(z,\, r,\, t)$ for $k = 1,\, 2,\, 3$ and $t(z,\, r,\, t_0)$. It is to be noted that the right sides of (3a) and (5) involve a'priori unknown roots of the nonlinear equation

$$t(z,r,t_0) = t$$

for t_0, where $t(z,\, r,\, t_0)$ is itself one of the scalar functions to be solved for. Nevertheless, it will be demonstrated in this section how the steady-state assumption enables Equations (3)–(6) to be solved for the field components as explicit nonlinear functionals of the electron arrival time.

Equations (3)–(7) are to be solved for $\boldsymbol{\mathcal{E}}_k(z,\, r,\, t)$ and $\boldsymbol{\mathcal{H}}_k(z,\, r,\, t)$, $k = 1,\, 2,\, 3$ and $t(z,\, r,\, t_0)$ subject to the sheath-helix boundary conditions, continuity conditions across the beam boundary, tangential electric field boundary conditions on the inner surface of the outer cylindrical shell, the monochromatic signalling conditions and the entrance conditions on the electron arrival time:

$$\begin{aligned}&\boldsymbol{\mathcal{E}}_1(z,1-,t)-\boldsymbol{\mathcal{E}}_1(z,1+,t)=0\\&\boldsymbol{\mathcal{E}}_1(z,1-,t)+\boldsymbol{\mathcal{E}}_2(z,1-,t)\cot\psi=0\\&\boldsymbol{\mathcal{E}}_1(z,1+,t)+\boldsymbol{\mathcal{E}}_2(z,1+,t)\cot\psi=0\\&\boldsymbol{\mathcal{H}}_1(z,1-,t)-\boldsymbol{\mathcal{H}}_1(z,1-,t)+[\boldsymbol{\mathcal{H}}_2(z,1-,t)-\boldsymbol{\mathcal{H}}_2(z,1+,t)]\cot\psi=0\end{aligned}\tag{8}$$

$$\left.\begin{aligned}&\boldsymbol{\mathcal{E}}_k(z,a-,t)-\boldsymbol{\mathcal{E}}_k(z,a+,t)=0\\&\boldsymbol{\mathcal{H}}_k(z,a-,t)-\boldsymbol{\mathcal{H}}_k(z,a+,t)=0\end{aligned}\right.\quad\text{for}\quad k=1,2,3\tag{9}$$

$$\boldsymbol{\mathcal{E}}_k(z,b-,t)=0\quad\text{for}\quad k=1,2,3\tag{10}$$

$$\begin{aligned}&\boldsymbol{\mathcal{E}}_1(0,1,t)=(A/2)\exp(jt)+c.c.\\&\boldsymbol{\mathcal{E}}_{1_z}(0,1,t)=-j\beta_1(A/2)\exp(jt)+c.c.\end{aligned}\tag{11}$$

$$\begin{aligned}&t(0,r,t_0)=t_0\\&t_z(0,r,t_0)=1\end{aligned}\tag{12}$$

In (8), ψ is the pitch angle of the sheath helix, $A(\triangleq\exp(j\theta))$ the phase factor of the input signal, $\beta_1(\triangleq v_0/v_p)$ the dimensionless phase shift constant of the cold-wave solution for the dielectric-loaded sheath helix at the operating radian frequency ω_0, and c.c. denotes the complex conjugate and for an arbitrary function *f(z, r, t)*

$$f(z,r_0\pm,t)\triangleq\lim_{\delta\downarrow 0}f(z,r_0\pm\delta,t)$$

In the definition of β_1, v_p is the phase speed of the axially symmetric cold-wave mode supported by the dielectric-loaded sheath helix at the angular frequency ω_0. The signalling conditions (11) imply that, in the immediate vicinity of $z=0$ and $r=1$ (i.e., of the helix boundary at the entrance plane), the solution for the field components corresponds to a forward traveling cold-wave. The convection current density and the electron charge density, along with the electromagnetic field components, are periodic functions of time in the steady state. They can hence be expanded in complex exponential Fourier series in t as

$$i(z,r,t)\;=\;q_0I_{[0,a]}(r)+\sum_{m=1}^{\infty}\left(i_m(z,r)\exp jmt+c.c.\right)\tag{13a}$$

$$\rho(z,r,t)\;=\;q_0I_{[0,a]}(r)+\sum_{m=1}^{\infty}\left(\rho_m(z,r)\exp jmt+c.c.\right)\tag{13b}$$

where, for any set B, I_B denotes its indicator function, defined as

$$I_B(X)=\begin{cases}1 & \text{if}\quad X\in B\\0 & \text{if}\quad X\notin B\end{cases}$$

and the 'Fourier coefficients' $i_m(z,r)$ and $\rho_m(z,r)$, $m\in N$, are given by

$$i_m(z,r)=(q_0/2\pi)\int_{-\pi}^{\pi}\left\{\sum_l\left|t_{t_0}(z,r,t_{0l}(z,r,t))\right|^{-1}\right\}\exp(-jmt)dt\tag{14a}$$

and

$$\rho_m(z,r)\;=\;(q_0/2\pi)\int_{-\pi}^{\pi}\left\{\sum_l t_z(z,r,t_{0l}(z,r,t))/\left|t_{t_0}(z,r,t_{0l}(z,r,t))\right|\right\}\exp(-jmt)dt\tag{14b}$$

where the symbol N denotes the set of natural numbers (positive integers).

Changing the variable of integration in (14) from t to t_0, with the substitution $t=t(z,r,t_0)$ and making use of change of variable formula for a many-to-one map established in Appendix A, we obtain

$$i_m(z,r)=(q_0/2\pi)\int_{-\pi}^{\pi}\exp(-jmt(z,r,t_0))dt_0\tag{15a}$$

and

$$\rho_m(z,r) = (q_0/2\pi)\int_{-\pi}^{\pi} t_z(z,r,t_0)\exp(-jmt(z,r,t_0))dt_0 \quad \text{for} \quad 0 \le z \le d \quad \text{and} \quad 0 \le r < a \tag{15b}$$

Thus we have represented the Fourier coefficients of $i(z,\, r,\, t)$ and $\rho(z,\, r,\, t)$ as nonlinear functionals of the electron-arrival time $t(z,\, r,\, t_0)$. These functional representations will play a crucial role in the large-signal field analysis the TWTA.

3. SOLUTION PROCEDURE

The solution of the nonlinear boundary value problem formulated in the previous section will be obtained in the following steps. A sequence of Green's functions (G_m), $m \ge 1$, with the mth Green's function G_m corresponding to the mth harmonic $m\omega_o$ of the input signal frequency, will be constructed for the slow-wave circuit. The axial electric field component inside the electron beam will then expressed as a nonlinear functional of the electron-arrival time through the above set of Green's functions. The expressions for all the electromagnetic field components will simultaneously be obtained in terms of the electron-arrival time.

Substitution of the expression for the axial electric field component inside the beam into the equation of electron motion puts the latter into the fixed-point format for a nonlinear operator on the Banach space of bounded continuous functions [16]. The unique solution for the fixed point problem for the electron arrival time may be obtained by successive approximations as guaranteed by the Banach fixed point theorem [16].

3.1. Construction of the Green's Functions

We start by expanding the field components, also in Fourier series, similarly to those in (13):

$$\left.\begin{aligned}\boldsymbol{\mathcal{E}}_k(z,r,t) &= E_{k0}(z,r)+\sum_{m=1}^{\infty}E_{km}(z,r)\exp(jmt)+c.c.\\ \boldsymbol{\mathcal{H}}_k(z,r,t) &= H_{k0}(z,r)+\sum_{m=1}^{\infty}H_{km}(z,r)\exp(jmt)+c.c.\end{aligned}\right\} \quad \text{for} \;\; k=1,2,3 \tag{16}$$

Substituting (16) together with (14) into the Maxwell's Equations (3)–(6), and equating the coefficients of $\exp(jmt)$, for $m \ge 0$, on both sides, we obtain

$$\begin{aligned} E_{10_z} + a_2\left(E_{30_r} + E_{30}/r\right) &= q_0 I_{[0,a]}(r)/a_1\\ E_{20_z} &= 0\\ E_{20_r} + E_{20}/r &= 0\\ E_{30_z} - a_2 E_{10_r} &= 0\end{aligned} \tag{17a}$$

$$\begin{aligned} H_{10_z} + a_2\left(H_{30_r} + H_{30}/r\right) &= 0\\ H_{20_z} &= 0\\ H_{20_r} + H_{20}/r &= q_0 I_{[0,a]}(r)/a_2\\ H_{30_z} - a_2 H_{10_r} &= 0\\ &\text{for} \quad m = 0\end{aligned} \tag{17b}$$

and

$$\left.\begin{aligned} &jma_1\kappa(r)E_{1m} - a_2\left(H_{2m_r} + H_{2m}/r\right) = -i_m(z,r)\\ &jma_1 H_{1m} + a_2\left(E_{2m_r} + E_{2m}/r\right) = 0\\ &jma_1\kappa(r)E_{2m} - H_{3m_z} + a_2 H_{1m_r} = 0\\ &jma_1 H_{2m} + E_{3m_z} - a_2 E_{1m_r} = 0\\ &jma_1\kappa(r)E_{3m} + H_{2m_z} = 0\\ &jma_1 H_{3m} - E_{2m_z} = 0\end{aligned}\right. \quad \text{for} \quad m \ge 1 \tag{18}$$

Equation (18) may be considered to be a nonhomogeneous system of partial differential equations for E_{km} and H_{km}, $k = 1, 2, 3$ with $-i_m(z, r)$ playing the role of the nonhomogeneous term. The equations corresponding to (5) and (6) do not appear in (18) as Maxwell's divergence Equations (5) and (6) are not independent of his curl Equations (3) and (4) for time-varying fields. The boundary conditions (8)–(10) and the signalling conditions (11), when expressed in terms of the Fourier coefficients, are

$$\begin{aligned}
&E_{1m}(z,1-) - E_{1m}(z,1+) = 0\\
&E_{1m}(z,1-) + E_{2m}(z,1-)\cot\psi = 0\\
&E_{1m}(z,1+) + E_{2m}(z,1+)\cot\psi = 0\\
&H_{1m}(z,1-) - H_{1m}(z,1+) + [H_{2m}(z,1-) - H_{2m}(z,1+)]\cot\psi = 0
\end{aligned} \tag{19a}$$

$$E_{km}(z,b-) = 0 \quad \text{for} \quad k = 1,2 \tag{19b}$$

$$\left.\begin{aligned}
&E_{km}(z,a-) - E_{km}(z,a+) = 0\\
&H_{km}(z,a-) - H_{km}(z,a+) = 0
\end{aligned}\right. \quad \text{for} \quad k = 1,2,3 \tag{19c}$$

$$\begin{aligned}
&E_{1m}(0,1) = (A/2)\delta_{1m}\\
&E_{1m_z}(0,1,) = -j\beta_1(A/2)\delta_{1m}
\end{aligned} \tag{19d}$$

where

$$\delta_{1m} = \begin{cases} 1 & \text{if} \quad m = 1 \\ 0 & \text{otherwise} \end{cases}$$

The solution of (17), satisfying the boundary and signalling conditions (19) for $m = 0$, is

$$\begin{aligned}
&E_{10} = H_{10} = E_{20} = H_{30} = 0\\
&H_{20} = a_1 E_{30} = q_0[rI_{[0,a]}(r) + a^2 I_{(a,b)}(r)/r]/2a_2
\end{aligned} \tag{20}$$

Now the solution of the nonhomogeneous boundary value problem described by (18) and (19) for $m \geq 1$ may be obtained as follows. The nonhomogeneous term $i_m(z, r)$ on the right side of (18) considered as a function of z, defined on the bounded interval $[0, d]$, is first expanded in a cosine series in the variable z:

$$i_m(z,r) = i_{mn}(r) + 2\sum_{n=-1}^{\infty} i_{mn}(r)\cos(jnk_d z) \quad \text{for} \quad 0 \leq z \leq d \tag{21}$$

where

$$k_d = 2\pi/d$$

and

$$i_{mn}(r) = (1/d)\int_0^d i_m(z,r)\cos(nk_d z)dz \tag{22}$$

Since $i_{m(-n)}(r) = i_{mn}(r)$, the cosine-series expansion (21) may be expressed in complex-exponential form as

$$i_m(z,r) = \sum_{n\in Z} i_{mn}(r)\exp(-jnk_d z) \quad \text{for} \quad 0 \leq z \leq d \tag{23}$$

In (23) and in the following, Z stands for the ring of integers. A solution of the boundary value problem described by (18) and (19), for each $m \geq 1$, is sought as a sum of two terms, the first term, the homogeneous solution, being a superposition of forward propagating and backward propagating cold waves (i.e., in absence of the electron beam) supported by the dielectric-loaded sheath and the second term being the 'particular' solution of the nonhomogeneous boundary value problem described by the partial differential Equation (18) and the boundary conditions (19a)–(19c). The particular solution for the phasor field components may be assumed to have the same form as the complex-exponential Fourier-series representation (23) of the nonhomogeneous term. The arbitrary constants appearing in the homogeneous solution are so chosen that the sum of the homogeneous and the particular solutions satisfies the signalling conditions (19d). Thus the solution for the phasor field components, for $m \geq 1$, may be represented as

$$\begin{aligned} E_{km}(z,r) &= E_{km}^{(h)}(z,r) + E_{km}^{(p)}(z,r) \\ &= E_{km}^{+}(r)\exp(-j\beta_m z) + E_{km}^{-}(r)\exp(j\beta_m z) + \sum_{n\in Z} E_{kmn}(r)\exp(-jnk_d z) \end{aligned} \tag{24a}$$

$$\begin{aligned} H_{km}(z,r) &= H_{km}^{(h)}(z,r) + H_{km}^{(p)}(z,r) \\ &= H_{km}^{+}(r)\exp(-j\beta_m z) + H_{km}^{-}(r)\exp(j\beta_m z) + \sum_{n\in Z} H_{kmn}(r)\exp(-jnk_d z) \end{aligned} \tag{24b}$$

$$\text{for} \quad 0 < z < d, \quad 0 \leq r < b \quad \text{and} \quad k = 1, 2, 3$$

where

$$E_{1m}^{\pm}(r) = A_m^{\pm} W_m(r) \tag{25a}$$
$$H_{1m}^{\pm}(r) = \left(-ja_2 A_m^{\pm} \tan\psi / ma_1\right) V_m(r) \tag{25b}$$
$$E_{2m}^{\pm}(r) = \left(-jma_1/a_2\tau_m^2(r)\right) H_{1m_r}^{\pm}(r) \tag{25c}$$
$$H_{3m}^{\pm}(r) = (\mp\beta_m/ma_1)E_{2m}^{\pm}(r) \tag{25d}$$
$$E_{3m}^{\pm}(r) = \left(\pm j\beta_m/a_2\tau_m^2(r)\right) E_{1m_r}^{\pm}(r) \tag{25e}$$
$$H_{2m}^{\pm}(r) = (\pm ma_1\kappa(r)/\beta_m)E_{3m}^{\pm}(r) \tag{25f}$$

In (25a) and (25b), $A_m^{\pm}$ are arbitrary constants of integration

$$W_m(r) \triangleq \begin{cases} [I_0(\tau_m r)/I_0(\tau_m)] & \text{for } 0 \leq r < 1 \\ [I_0(\tilde{\tau}_m r) - \sigma_m K_0(\tilde{\tau}_m r)]/[I_0(\tilde{\tau}_m) - \sigma_m K_0(\tilde{\tau}_m)] & \text{for } 1 < r < b \end{cases} \tag{26a}$$

$$V_m(r) \triangleq \begin{cases} [\tau_m I_0(\tau_m r)/I_0'(\tau_m)] & \text{for } 0 \leq r < 1 \\ \tilde{\tau}_m[I_0(\tilde{\tau}_m r) - \sigma_m' K_0(\tilde{\tau}_m r)]/[I_0'(\tilde{\tau}_m) - \sigma_m' K_0'(\tilde{\tau}_m)] & \text{for } 1 < r < b \end{cases} \tag{26b}$$

where

$$\begin{aligned} \tau_m^2 &= \left[\beta_m^2 - m^2 a_1^2\right]/a_2^2 \\ \tilde{\tau}_m^2 &= \left[\beta_m^2 - m^2 a_1^2 \varepsilon_{\mathit{eff}}\right]/a_2^2 \end{aligned} \tag{27a}$$

and the function $\tau_m(r)$ appearing in (25c) and (25e) is defined in terms of τ_m and $\tilde{\tau}_m$ by

$$\tau_m^2(r) = \tau_m^2 I_{[0,1]}(r) + \tilde{\tau}_m^2 I_{(1,b)}(r) = \left[\beta_m^2 - \kappa(r) m^2 a_1^2\right]/a_2^2 \tag{27b}$$

In (27b)

$$\sigma_m \underline{\Delta} I_0(\tilde{\tau}_{mb})/K_0(\tilde{\tau}_{mb}), \quad \sigma_m' \underline{\Delta} I_0'(\tilde{\tau}_{mb})/K_0'(\tilde{\tau}_{mb}) \tag{28}$$

and the abbreviation $\tilde{\tau}_{mb} = \tilde{\tau}_m b$ has been used in the definitions (28). The phase-shift constants $\beta_m(> 0)$ of the cold wave supported by the dielectric-loaded sheath helix at the radian frequency $m\omega_0$ satisfies the dispersion equation

$$\begin{aligned} &\tau_m I_0(\tau_m)/I_1(\tau_m) + \tilde{\tau}_m \Delta_{m10}(1)/\Delta_{m11}(1) \\ &= (ma_1 \cot\psi/a_2)^2 \left(I_1(\tau_m)/\tau_m I_0(\tau_m) + \varepsilon_{\mathit{eff}} \Delta_{m01}(1)/\tilde{\tau}_m \Delta_{m00}(1)\right) \end{aligned} \tag{29}$$

where

$$\begin{aligned} \Delta_{m11}(r) &= I_1(\tilde{\tau}_{mb})K_1(\tilde{\tau}_m r) - K_1(\tilde{\tau}_{mb})I_1(\tilde{\tau}_m r) \\ \Delta_{m10}(r) &= I_1(\tilde{\tau}_{mb})K_0(\tilde{\tau}_m r) + K_1(\tilde{\tau}_{mb})I_0(\tilde{\tau}_m r) \\ \Delta_{m01}(r) &= I_0(\tilde{\tau}_{mb})K_1(\tilde{\tau}_m r) + K_0(\tilde{\tau}_{mb})I_1(\tilde{\tau}_m r) \\ \Delta_{m00}(r) &= I_0(\tilde{\tau}_{mb})K_0(\tilde{\tau}_m r) - K_0(\tilde{\tau}_{mb})I_0(\tilde{\tau}_m r) \end{aligned} \tag{30}$$

In (26), (28), (29), (30) and henceforth, I_v and K_v, $v = 0, 1, 2, \ldots$ denote vth order modified Bessel function of the first and second kind respectively.

The expressions for $E_{kmn}(r)$ and $H_{kmn}(r)$, $k = 1, 2, 3$ and $n \in Z$, appearing as Fourier coefficients in the Fourier-series representation of the particular solution to the nonhomogeneous boundary value problem described by (18) and (19a)–(19c) are

$$E_{1mn}(r) = \begin{cases} (j/ma_1 d)\int_0^d\int_0^a G_{mn}(r,y))i_m(x,y)(\cos nk_d x)ydydx & \text{if } \tau_{mn}^2(r)\neq 0 \\ 0 & \text{if } \tau_{mn}^2=0 \text{ or } \tilde{\tau}_{mn}^2=0 \end{cases} \quad \text{for } 0\le r<b \tag{31a}$$

$$H_{1mn}(r) = \begin{cases} \left(a_2\tan\psi/m^2a_1^2 d\Lambda_{mn}C_0(p_{mn})\right)\int_0^d\int_0^a V_{mn}(r)C_0(p_{mn}y)i_m(x,y)(\cos nk_d x)ydydx \\ \qquad\qquad \text{if } \tau_{mn}^2(r)\neq 0 \\ 0 \qquad\qquad \text{if } \tau_{mn}^2=0 \text{ or } \tilde{\tau}_{mn}^2=0 \end{cases} \quad \text{for } 0\le r<b \tag{31b}$$

$$E_{2mn}(r) = \left(-jma_1/a_2\tau_{mn}^2(r)\right)H_{1mn_r}(r) \quad \text{for} \quad 0\le r<b \tag{31c}$$

$$H_{2mn}(r)=\begin{cases} \left(jma_1\kappa(r)/a_2\tau_{mn}^2(r)\right)E_{1mn_r}(r) & \text{if} \quad \tau_{mn}^2(r)\neq 0 \\ (1/a_2dr)\int_0^d\int_0^{r\wedge a} i_m(x,y)(\cos\, nk_d x\,)ydydx & \text{if} \quad \tau_{mn}^2=0 \\ 0 & \text{if} \quad \tilde{\tau}_{mn}^2=0 \end{cases} \quad \text{for} \quad 0\le r<b \tag{31d}$$

$$H_{3mn}(r)=(-nk_d/ma_1)\,E_{2mn}(r) \quad \text{for} \quad 0\le r<b \tag{31e}$$

$$E_{3mn}(r)=\begin{cases}(nk_d/ma_1\kappa(r))\,H_{2mn}(r) & \text{if } \tau_{mn}^2\neq 0 \\ (nk_d/ma_1)\,H_{2mn}(r) & \text{if } \tau_{mn}^2=0\end{cases} \quad \text{for } 0\le r<b \tag{31f}$$

where the partial Green's function $G_{mn}(r,\,y)$, defined on $[0,b)\times[0,a]$, is given by

$$G_{mn}(r,y)=\begin{cases}\tau_{mn}^2\{D_0(p_{mn}r)C_0(p_{mn}y)I_{[0,r\wedge a]}(y)+C_0(p_{mn}r)D_0(p_{mn}y)I_{[r\wedge a,a]}(y) \\ \quad -D_0(p_{mn})C_0(p_{mn}r)C_0(p_{mn}y)/C_0(p_{mn})\}+C_0(p_{mn}r)C_0(p_{mn}y)/\Lambda_{mn}C_0^2(p_{mn}) \\ \qquad\qquad\qquad\qquad \text{for } 0\le r\le 1 \\ (C_0(\tilde{p}_{mn}r)-\sigma_{mn}D_0(\tilde{p}_{mn}r))/\Lambda_{mn}C_0(p_{mn})(C_0(\tilde{p}_{mn})-\sigma_{mn}D_0(\tilde{p}_{mn})) \quad \text{for } 1<r<b\end{cases} \tag{32}$$

and

$$V_{mn}(r)=\begin{cases}p_{mn}C_0(p_{mn}r)/C_1(p_{mn}) & \text{for} \quad 0\le r<1 \\ \tilde{p}_{mn}(C_0(\tilde{p}_{mn}r)-\sigma'_{mn}D_0(\tilde{p}_{mn}r))/((C_1(\tilde{p}_{mn})+\sigma'_{mn}D_1(\tilde{p}_{mn})) & \text{for} \quad 1<r<b\end{cases} \tag{33}$$

In (31), (32) and in the following

$$\begin{aligned}\Lambda_{mn} &= \left[(a_2\tan\psi/ma_1)^2\left\{\frac{p_{mn}C_0(p_{mn})}{C_1(p_{mn})}+\frac{\tilde{p}_{mn}\Delta_{mn10}}{\Delta_{mn11}}\right\}-\frac{C_1(p_{mn})}{p_{mn}C_0(p_{mn})}-\frac{\varepsilon_{\mathit{eff}}\Delta_{mn01}}{\Delta_{mn00}}\right] \\ \tau_{mn}^2 &= \left[n^2k_d^2-m^2a_1^2\right]/a_2^2 \\ \tilde{\tau}_{mn}^2 &= \left[n^2k_d^2-\varepsilon_{\mathit{eff}}m^2a_1^2\right]/a_2^2\end{aligned} \tag{34}$$

and

$$\tau_{mn}^2(r)\triangleq\left[nk_d^2-m^2a_1^2\kappa(r)\right]/a_2^2=\begin{cases}\tau_{mn}^2 & \text{for} \quad 0\le r<1 \\ \tilde{\tau}_{mn}^2 & \text{for} \quad 1<r<b\end{cases}$$

$$p_{mn}\triangleq|\tau_{mn}|, \quad \tilde{p}_{mn}\triangleq|\tilde{\tau}_{mn}|, \quad r\wedge a=\min(r,a)$$

and where

$$\begin{aligned}\sigma_{mn} &= C_0(\tilde{p}_{mn}b)/D_0(\tilde{p}_{mn}b),\\ \sigma'_{mn} &= C'_0(\tilde{p}_{mn}b)/D'_0(\tilde{p}_{mn}b) = -C_1(\tilde{p}_{mn}b)/D_1(\tilde{p}_{mn}b)\end{aligned} \tag{35a}$$

$$\begin{aligned}\Delta_{mn11} &= C_1(\tilde{p}_{mn}b)D_1(\tilde{p}_{mn}) - D_1(\tilde{p}_{mn}b)C_1(\tilde{p}_{mn})\\ \Delta_{mn10} &= C_1(\tilde{p}_{mn}b)D_0(\tilde{p}_{mn}) + D_1(\tilde{p}_{mn}b)C_0(\tilde{p}_{mn})\\ \Delta_{mn01} &= C_0(\tilde{p}_{mn}b)D_1(\tilde{p}_{mn}) + D_0(\tilde{p}_{mn}b)C_1(\tilde{p}_{mn})\\ \Delta_{mn00} &= C_0(\tilde{p}_{mn}b)D_0(\tilde{p}_{mn}) - D_0(\tilde{p}_{mn}b)C_0(\tilde{p}_{mn})\end{aligned} \tag{35b}$$

In (31b), (32)–(34) and (35) and in the following, we have denoted the Bessel functions and the modified Bessel functions (of integer order) appearing for the positive and negative values of τ^2_{mn} and $\tilde{\tau}^2_{mn}$ using a common symbol as follows:

$$\begin{aligned}C_v(p_{mn}r) &= J_v(p_{mn}r) \quad \text{if} \quad \tau^2_{mn} < 0\\ & I_v(p_{mn}r) \quad \text{if} \quad \tau^2_{mn} > 0\\ D_v(p_{mn}r) &= (-1)^{v+1}(\pi/2)Y_v(p_{mn}r) \quad \text{if} \quad \tau^2_{mn} < 0\\ & K_v(p_{mn}r) \qquad\qquad\qquad \text{if} \quad \tau^2_{mn} > 0\\ &\text{for} \quad v = 0, 1, 2, \ldots \quad \text{and for} \quad 0 \leq r < 1\end{aligned} \tag{36}$$

where J_v and Y_v, $v = 0,\ 1,\ 2,\ \ldots.$ denote vth order (ordinary) Bessel functions of the first and second kind respectively.

For $1 < r < b$, the corresponding $C_v(\tilde{p}_{mn}r)$ and $D_v(\tilde{p}_{mn}r)$ are also defined by the right side of (36) except for the replacement of p_{mn} by $\tilde{p}_{mn}$ and τ^2_{mn} by $\tilde{\tau}^2_{mn}$. In arriving at the formulas (31a) and (31b) for $E_{1mn}(r)$ and $H_{1mn}(r)$, we have made use of (22). Finally, the arbitrary constants $A^{\pm}_m$, $m \geq 1$, appearing in the homogeneous part of the solution (25) are chosen so that the sum of homogeneous and nonhomogeneous parts of the solution satisfies the signalling conditions (19d). Thus

$$\begin{aligned}A^+_m &= A\delta_{1m}/2 - \sum_{n\in\mathbb{Z}} E_{1mn}(1)/2\\ A^-_m &= -\sum_{n\in\mathbb{Z}} E_{1mn}(1)/2\end{aligned} \tag{37}$$

Writing down the particular solution (31) for the Fourier coefficients of the field components and the formula for $G_{mn}(r, y)$, we have tacitly assumed that $\Lambda_{mn} \neq 0$ for all $m \in N$ and $n \in Z$. Since Λ_{mn} cannot vanish for $0 \leq |n| < ma_1/k_d$, we require specifically that τ_{mn} for $|n| > ma_1/k_d$ does not coincide with τ_m for any $m \geq 1$ or equivalently that $\beta_m \neq |n|k_d$ for any $m \in N$ and $n \in Z$; the condition for non-resonance. The modifications required in the form of the solution and in the expressions for the Green's functions, when there is resonance, are relegated to Appendix B, so as not to interrupt the main stream of the development at this stage.

Incorporating the values of the arbitrary constants $A^{\pm}_m$ given by (37) into (25), the homogeneous part of the solution for the field components may be represented in the non-resonant case in the form

$$E^{(h)}_{1m}(z, r) = \delta_{1m}(A/2)W_1(r)\exp(-j\beta_1 z) - (j/ma_1 d)W_m(r)\cos\beta_m z \int_0^d\!\!\int_0^a U_m(x, y)i_m(x, y)y\,dy\,dx \tag{38a}$$

$$\begin{aligned}H^{(h)}_{1m}(z, r) &= (-ja_2\tan\psi/ma_1)\delta_{1m}(A/2)V_1(r)\exp(-j\beta_1 z)\\ &\quad - \left(a_2\tan\psi/m^2a_1^2 d\right)V_m(r)\cos\beta_m z \int_0^d\int_0^a U_m(x, y)i_m(x, y)y\,dy\,dx\end{aligned} \tag{38b}$$

$$E^{(h)}_{2m}(z, r) = \left(-jma_1/a_2\tau^2_m(r)\right) H^{(h)}_{1m_r}(z, r) \tag{38c}$$

$$H^{(h)}_{2m}(z, r) = \left(jma_1\kappa(r)/a_2\tau^2_m(r)\right) E^{(h)}_{1m_r}(z, r) \tag{38d}$$

$$E_{3m}^{(h)}(z,r)=(j/ma_1^2\kappa(r))H_{2m_z}^{(h)}(z,r) \tag{38e}$$

$$H_{3m}^{(h)}(z,r)=(-j/ma_1)E_{2m_z}^{(h)}(z,r) \quad \text{for} \quad 0 \le r < b, \quad 0 \le z \le d \tag{38f}$$

where

$$U_m(x,y) \triangleq \sum_{n \in Z} (\cos nk_d x \; C_0(p_{mn}y)/\Lambda_{mn}C_0(p_{mn})) \tag{39}$$

The complete solution for the field components is then obtained (in the non-resonant case) by combining the homogeneous part given by (38) with the Fourier-series representation of the nonhomogeneous part according to (24) after substituting for the 'Fourier coefficients' from (31). In order to derive the nonlinear integral equation satisfied the electron-arrival time $t(z, r, t_0)$, it is first necessary to express the axial electric field component inside the electron beam as an explicit nonlinear functional of $t(z, r, t_0)$ through a Green's function sequence $G_m(z, r; x, y)$, $m \ge 1$, for the dielectric-loaded sheath helix. Substituting for $E_{1m}^{(h)}(z,r)$ and $E_{1mn}(r)$, $n \in Z$, from (38a) and (31a) into the representation

$$E_{1m}(z,r) = E_{1m}^{(h)}(z,r) + \sum_{n \in Z} E_{1mn}(r) \exp(-jnk_d z) \tag{40}$$

for the axial phasor electric field component and making use of the formula (15a) for $i_m(z,r)$, the axial (physical) electric field component

$$\boldsymbol{\mathcal{E}}_1(z,r,t) = \sum_{m=1}^{\infty} E_{1m}(z,r) \exp(-jmt) + c.c$$

may be represented as

$$\begin{aligned}\boldsymbol{\mathcal{E}}_1(z,r,t) \; &= \; \delta_{1m} W_1(r) \left((A/2) \exp(j(t-\beta_1 z)) + c.c\right) + (jq_0/2\pi a_1 d) \\ &\sum_{m=1}^{\infty} (1/m) \exp(jmt) \int_0^d dx \int_0^a G_m(z,r;x,y) y dy \int_{-\pi}^{\pi} \exp\{-jmt(x,y,\tau)\} d\tau + c.c.\end{aligned} \tag{41}$$

where the mth Green's function

$$G_m(z,r;x,y) = \sum_{n \in Z} [G_{mn}(r,y) \exp(-jnk_d z) - W_m(r) G_{mn}(1,y) \cos \beta_m z] \cos nk_d x \tag{42}$$

and from (32)

$$G_{mn}(1,y) = \; C_0(p_{mn}y)/\Lambda_{mn} C_0(p_{mn})$$

This concludes the construction of the Green's function sequence $G_m(z, r; x, y)$, $m \ge 1$, for the slow-wave structure.

3.2. Reduction to the Fixed-point Problem and the Method of Successive Approximations

Formal integration of (7) with the help of the entrance conditions (12) gives

$$t(z,r,t_0) = t_0 + \int_0^z dx / \left\{ 1 - 2\varepsilon \int_0^x \boldsymbol{\mathcal{E}}_1(s,r,t(s,r,t_0)) ds \right\}^{1/2} \quad \text{for} \quad 0 \le z \le d \quad \text{and} \quad 0 \le r \le a \tag{43}$$

where $\boldsymbol{\mathcal{E}}_1(z, r, t)$ was defined in (16) and is represented as a nonlinear functional of the electron-arrival time $t(z, r, t_0)$ in (41). In terms of the electron transit-time $\theta(z,r,t_0)(\triangleq t(z,r,t_0) - t_0)$, (43) reads

$$\theta(z,r,t_0) = \int_0^z dx / \left\{ 1 - 2\varepsilon \int_0^x F(s,r,t_0,\theta(s,r,t_0)) ds \right\}^{1/2} \tag{44}$$

where

$$F(s,r,t_0,\theta(s,r,t_0)) \triangleq \boldsymbol{\mathcal{E}}_1(z,r,t_0+\theta(z,r,t_0))$$

Consider now the Banach space $C(D)$ of bounded continuous (real-valued) functions $\theta(z,\, r,\, t_0)$ defined on the region

$$D \triangleq \{(z, r, t_0) : \quad 0 \leq z \leq d, \quad 0 \leq r \leq a, \quad -\pi \leq t_0 \leq \pi\}$$

with norm

$$\|\theta\| \triangleq \max_{(z,r,t_0)\in D} |\theta(z, r, t_0)|$$

Let T be the operator mapping $C(D)$ into $C(D)$, defined by the right side of (44). Equation (44) then becomes a fixed-point statement for the operator T. Let $\theta_0 \in C(D)$ be arbitrary (it is expedient to take $\theta_0 = z$ in numerical evaluation of the fixed point). Starting with θ_0 as the initial approximation, we recursively define a sequence of successive approximations by

$$\theta_n = T(\theta_{n-1}) \quad \text{for} \quad n \geq 1 \tag{45}$$

It is straightforward to check that each $\theta_n (n \geq 1)$ is well defined. That the sequence of successive approximations $(\theta_n)_{n\geq 0}$ converges to the unique fixed point of T in the Banach space $C(D)$ is guaranteed by the classical Banach fixed point theorem [16]. That the operator T is a contraction for sufficiently small ε is demonstrated in [17]. Once the functional form of $t(z,\, r,\, t_0)$ has been identified, the solution for all the field components readily follow.

4. CONCLUDING COMMENTS

We have thus demonstrated, as for the case of the open sheath-helix model for the slow-wave structure [11–13], the feasibility of a rigorous large-signal field analysis of a linear beam travelling wave tube amplifier for the more practically relevant model of dielectric-loaded sheath helix. Numerical computation of TWTA parameters such as the power gain, current gain, conversion efficiency, optimum interaction length etc. on the basis of the large signal field theory developed in this paper will be presented in the second part of this contribution.

It is, however, far from clear as to what extent the proposed set of signalling conditions simulates the input conditions in a traveling wave tube. In practice the two ends of a tape helix (of finite length, finite ribbon thickness and finite material conductivity) are transformed to the shape of circular cylindrical conductors which are then extended outside the tube to form the central conductors of coaxial transmission lines through which r.f. power is coupled in and out of the tube. Unfortunately the sheath-helix model of the slow-wave structure is incompatible with this coupling arrangement. For this reason it is impossible to rigorously account for the perturbation of the field configuration due to the input and the output connections within the framework of the sheath-helix model. In this context, it will be of interest to model the slow-wave structure to be a finite-length tape helix which is indeed compatible with input and output coupling arrangements employing shielded strip lines to carry microwave power into and out of the TWTA.

Work on a large-signal field theory for a linear beam travelling wave tube amplifier (TWTA) making use of the dielectric-loaded tape-helix model analysed in [20] for the slow-wave structure is in progress and will be reported in due course.

APPENDIX A.

In this appendix, we give a proof of the change-of-variables formula used to arrive expressions (15) for the Fourier coefficients $i_m(z,r)$ and $\rho_m(z,r)$, $m \in N$.

Let X be an absolutely continuous random variable with density p_X. Let another random variable Y be defined by $Y = g(X)$ where g is a differentiable but not necessarily one-to-one function. The density of Y is then given in terms of that X by [18]

$$p_Y(y) = \sum_l p_X(x_l(y))/|dg(x_l(y))/dx| \tag{A1}$$

where the summation is over all the roots $x_l(y)$ (at most countable) of the equation $g(x) = y$ for x. Now for any Borel function f [19], the expectation of $f(X)$, by definition, is

$$Ef(Y) \triangleq \int_R f(y)p_Y(y)dy \tag{A2}$$

In terms of the density p_X of the random variable X, (A2) may be expressed as [19]

$$Ef(Y) = Efog(X) = \int_R f(g(x))p_X(x)dx \tag{A3}$$

On substituting for $p_X(x)$ from (A1) and equating the two expressions for $Ef(Y)$, we have

$$\int_R f(y)\left(\sum_l p_X(x_l(y))/|dg(x_l(y))/dx|\right)dy = \int_R f(g(x))p_X(x)dx \tag{A4}$$

Setting $x = t_0$, $y = t$, $g(\cdot) = t(z,r,\cdot)$, $f(\cdot) = (q_0/2\pi)\exp(-jm\ \cdot)$ and choosing successively $p_X(\cdot) = I_{[-\pi,\pi]}(\cdot)/2\pi$ and $p_X(\cdot) = t_z(z,r,\ \cdot)I_{[-\pi,\pi]}(\cdot)/\int_{-\pi}^{\pi} t_z(z,r,\ \tau)d\tau$ in (A4), we obtain the change-of-variables formulas

$$(q_0/2\pi)\int_{g([-\pi,\pi])}\left(\sum_l |t_{t_0}(z,r,t_{0l}(z,r,t))|^{-1}\right)\exp(-jmt)dt = (q_0/2\pi)\int_{-\pi}^{\pi}\exp(-jmt(z,r,t_0))dt_0 \tag{A5a}$$

and

$$(q_0/2\pi)\int_{g([-\pi,\pi])}\left(\sum_l t_z(z,r,t_{0l}(z,r,t))/|t_{t_0}(z,r,t_{0l}(z,r,t))|\right)\exp(-jmt)dt$$
$$= (q_0/2\pi)\int_{-\pi}^{\pi} t_z(z,r,t_0)\exp(-jmt(z,r,t_0))dt_0 \tag{A5b}$$

Since the image $g[-\pi,\ \pi]$ of the interval $[-\pi,\pi]$ under the map g is again an interval of length 2π and the integrands on the left sides of (A5a) and (A5b) are 2π-periodic in the variable t, we recover the expressions (15a) and (15b) for the Fourier coefficients $i_m(z,r)$ and $\rho_m(z,r)$.

APPENDIX B.

In this appendix, we give the modifications required in the form of the particular solution $E_{km}(z,r)$ and $H_{km}(z,\ r)$, $k = 1,\ 2,\ 3$, for the phasor field components, when there exist integers m and n (with $m \geq 1$ and $|n| > ma_1/k_d$) for which

$$\tau_{mn} = \tau_m$$

or equivalently

$$nk_d = \pm\beta_m \tag{B1}$$

When the condition (B1) for resonance is satisfied, the Λ_{mn} appearing in the particular solution (31) for $E_{kmn}(r)$ and $H_{kmn}(r)$, $k = 1,\ 2,\ 3$, (implicitly through the expression (32) for the partial Green's function $G_{mn}(r,\ y)$ in the case of $E_{1mn}(r)$) becomes zero and the solution (31) loses its validity. It is to be noted that resonance is possible if and only if the set

$$Q \triangleq \{m \in N : \exists\ n \in N \quad \text{with} \quad nk_d = \beta_m\}$$

is nonempty. Physically, the condition (B1) means that the interaction length of the TWTA is an integral multiple of a cold wavelength at the mth harmonic of the input signal frequency. In this resonant case, the particular solution for the nonhomogeneous boundary value problem described by (18) and (19a)–(19c) has to be assumed in the alternate form

$$\begin{aligned} E_{km}(z,r) &= \sum_{n\in\mathbb{Z}} \left(\varepsilon_{mn} z \bar{E}_{kmn}(r) + E_{kmn}(r)\right) \exp(-jnk_d z) \\ H_{km}(z,r) &= \sum_{n\in\mathbb{Z}} \left(\varepsilon_{mn} z \bar{H}_{kmn}(r) + H_{kmn}(r)\right) \exp(-jnk_d z) \\ &\qquad\qquad \text{for} \quad k=1,2,3 \end{aligned} \tag{B2}$$

where

$$\varepsilon_{mn} = \begin{cases} 1 & \text{whenever} \quad nk_d = \pm\beta_m \\ 0 & \text{otherwise} \end{cases}$$

We will now obtain the expressions for $\bar{E}_{kmn}(r)$, $\bar{H}_{kmn}(r)$, $E_{kmn}(r)$ and $H_{kmn}(r)$ assuming that the resonance condition (B1) is satisfied by the pair of integers m and n. Substituting (B2) into (18) and (19a)–(19c), equating firstly the coefficients of $\exp(-jnk_d z)$ and then the coefficients of z^p for $p = 1$ and 0 on both sides, we obtain ordinary differential equations and corresponding boundary conditions to be satisfied the functions $\bar{E}_{kmn}(r)$, $\bar{H}_{kmn}(r)$, $E_{kmn}(r)$ and $H_{kmn}(r)$. The solution of the homogeneous system of differential equations for $\bar{E}_{kmn}(r)$ and $\bar{H}_{kmn}(r)$ satisfying the corresponding boundary conditions, is given by (25) except that the arbitrary constants $A_m^{\pm}$ appearing therein are denoted by $\bar{A}_{mn}(n = \pm\beta_m/k_d)$ in the present context. The solution of the nonhomogeneous system of ordinary differential equations for $E_{kmn}(r)$ and $H_{kmn}(r)$ for $k = 1, 2, 3$, that is continuous across the beam boundary at $r = a$ and consistent with the tangential electric field boundary conditions $E_{kmn}(b) = 0$ for $k = 1, 2$, at the inner surface of the outer cylindrical conductor may be expressed as

$$E_{1mn}(r) = \begin{cases} I_0(\tau_m r) A_{mn} - (j\tau_m^2/ma_1) \displaystyle\int_0^{r\wedge a} \tilde{G}_m(r,y) i_{mn}(y) y\,dy \\ + (2jnk_d/a_2^2 I_0(\tau_m)) \bar{A}_{mn} \displaystyle\int_0^{r} \tilde{G}_m(r,y) I_0(\tau_m y) y\,dy \quad \text{for } 0 \le r < 1 \\ \Delta_{m00}(r) C_{mn}/K_0(\tilde{\tau}_{mb}) + \left(2jnk_d \varepsilon_{\mathit{eff}}/a_2^2 \Delta_{m00}(1)\right) \\ \bar{A}_{mn} \displaystyle\int_r^{b} \tilde{G}_m(r,y) \Delta_{m00}(y) y\,dy \quad \text{for } 1 < r < b \end{cases} \tag{B3a}$$

$$H_{1mn}(r) = \begin{cases} I_0(\tau_m r) B_{mn} - (2nk_d m a_1 \tau_m \tan\psi/a_2 I_1(\tau_m)) \\ \bar{A}_{mn} \displaystyle\int_0^{r} \tilde{G}_m(r,y) I_0(\tau_m y) y\,dy \quad \text{for} \quad 0 \le r < 1 \\ \Delta_{m10}(r) D_{mn}/K_1(\tilde{\tau}_{mb}) + (2nk_d m a_1 \tau_m \tan\psi/a_2 \Delta_{m11}(1)) \\ \bar{A}_{mn} \displaystyle\int_r^{b} \tilde{G}_m(r,y) \Delta_{m10}(y) y\,dy \quad 1 < r < b \end{cases} \tag{B3b}$$

$$E_{2mn}(r) = \left(-jma_1/a_2\tau_m^2(r)\right) H_{1mn_r}(r) \tag{B3c}$$

$$H_{2mn}(r) = \left(jma_1\kappa(r)/a_2\tau_m^2(r)\right) E_{1mn_r}(r) \tag{B3d}$$

$$E_{3mn}(r) = (nk_d/ma_1\kappa(r)) H_{2mn}(r) - e_{m1}(r)\bar{A}_{mn}/a_2\tau_m(r) \tag{B3e}$$

$$H_{3mn}(r) = (-nk_d/ma_1) E_{2mn}(r) - jh_{m1}(r)\bar{A}_{mn}\tan\psi/ma_1 \tag{B3f}$$

where

$$\begin{aligned}\tilde{G}_m(r,y) &\triangleq I_0(\tau_m r)K_0(\tau_m y) - K_0(\tau_m r)I_0(\tau_m r) \quad \text{for} \quad 0 \le y \le r \le 1\\ &\quad K_0(\tilde{\tau}_m r)I_0(\tilde{\tau}_m y) - I_0(\tilde{\tau}_m r)K_0(\tilde{\tau}_m r) \quad \text{for} \quad 1 < r \le y \le b\\ e_{mi}(r) &= I_i(\tau_m r)/I_0(\tau_m) \quad \text{for} \quad 0 \le r < 1\\ &\quad \Delta_{m0i}(\tau_m)/\Delta_{m00}(1) \quad \text{for} \quad 1 < r < b, \quad i = 0, 1\\ h_{mi}(r) &= I_i(\tau_m r)/I_1(\tau_m) \quad \text{for} \quad 0 \le r < 1\\ &\quad \Delta_{m1i}(\tau_m)/\Delta_{m11}(1) \quad \text{for} \quad 1 < r < b, \quad i = 0, 1\end{aligned}$$

The arbitrary constants B_{mn}, C_{mn} and D_{mn} can be determined in terms of A_{mn} and $\bar{A}_{mn}$ using the first three sheath-helix boundary conditions:

$$\begin{aligned}C_{mn} &= I_0(\tau_m)K_0(\tilde{\tau}_{mb})A_{mn}/\Delta_{m00}(1) - \left(j\tau_m^2 K_0(\tilde{\tau}_{mb})/ma_1\Delta_{m00}(1)\right)\int_0^a \tilde{G}_m(1,y)i_{mn}(y)ydy\\ &\quad + \left(jnk_d K_0(\tilde{\tau}_{mb})/a_2^2\Delta_{m00}(1)\right)[I_1(\tau_m)/\tau_m I_0(\tau_m)\\ &\quad + \varepsilon_{\mathit{eff}}\Delta_{m01}(1)(1-b\Delta_{m10}(1)/\Delta_{m01}(1))/\tilde{\tau}_m\Delta_{m00}(1)]\bar{A}_{mn} \qquad \text{(B4a)}\end{aligned}$$

$$\begin{aligned}B_{mn} &= \left(-ja_2\tau_m I_0(\tau_m)\tan\psi/ma_1 I_1(\tau_m)\right)A_{mn} - \left(\tau_m^3 a_2\tan\psi/(ma_1)^2 I_1(\tau_m)\right)\int_0^a \tilde{G}_m(1,y)i_{mn}(y)ydy\\ &\quad + nk_d\tan\psi\left(1+m^2a_1^2 I_0^2(\tau_m)/I_1^2(\tau_m)\right)\bar{A}_{mn}/ma_1a_2I_0(\tau_m) \qquad \text{(B4b)}\end{aligned}$$

$$\begin{aligned}D_{mn} &= ja_2\tilde{\tau}_m K_1(\tilde{\tau}_{mb})I_0(\tau_m)A_{mn}\tan\psi/ma_1\Delta_{m11}(1)\\ &\quad + \left(a_2\tau_m^2\tilde{\tau}_m K_1(\tilde{\tau}_{mb})\tan\psi/m^2a_1^2\Delta_{m11}(1)\right)\int_0^a \tilde{G}_m(1,y)i_{mn}(y)ydy\\ &\quad - \left(nk_d K_1(\tilde{\tau}_{mb})\tan\psi/ma_1a_2\Delta_{m11}(1)\right)[\tilde{\tau}_m I_1(\tau_m)/\tau_m I_0(\tau_m)\\ &\quad - m^2a_1^2\Delta_{m10}(1)(1-b\Delta_{m01}(1)/\Delta_{m10}(1))/\Delta_{m11}(1)]\bar{A}_{mn} \qquad \text{(B4c)}\end{aligned}$$

Finally substituting for $H_{1mn}(1\pm)$ and $H_{2mn}(1\pm)$ from (B3b) and (B3d) into the fourth sheath-helix boundary condition and making use of the relations (B4), the fourth boundary condition may be manipulated into the form

$$\begin{aligned}&\left(-jma_1I_0(\tau_m)\Lambda_{mn}\cot\psi/a_2\right)A_{mn} + \left(ma_1nk_d\cot\psi/a_2\right)\left[\left(I_1^2(\tau_m)/I_0^2(\tau_m)-1\right)/a_2^2\tau_m^2\right.\\ &+\left(I_0^2(\tau_m)/I_1^2(\tau_m)-1\right)\tan^2\psi\nabla+\left(1+\tilde{\tau}_m^{-2}\Delta_{m11}^{-2}(1)-\Delta_{m10}^2(1)/\Delta_{m11}^2(1)\right)\tan^2\psi+\varepsilon_{\mathit{eff}}\left(1+\tilde{\tau}_m^{-2}\Delta_{m00}^{-2}(1)\right.\\ &\left.\left.-\Delta_{m01}^2(1)/\Delta_{m00}^2(1)\right)/a_2^2\tilde{\tau}_m^2\right]\bar{A}_{mn} + \left(\cot\psi/a_2I_0(\tau_m)\right)\int_0^a I_0(\tau_m y)i_{mn}(y)ydy = 0 \qquad \text{(B5)}\end{aligned}$$

The sheath helix dispersion Equation (29) has been used repeatedly in order to arrive at the form (B5) of the fourth sheath-helix boundary condition. Since the resonance condition (B1) has been assumed to be met by the integer pair (m,n), $\Lambda_{mn} = 0$. Hence a solution for $\bar{A}_{mn}$ exists only if the solvability condition

$$\bar{A}_{mn} = \left(\mathrm{sgn}(n)/ma_1\beta_m\Delta_m\right)\int_0^a \left(I_0(\tau_m y)/I_0(\tau_m)\right)i_{mn}(y)ydy \qquad \text{(B6)}$$

is satisfied where

$$\begin{aligned}\Delta_m &\triangleq \left(1-I_1^2(\tau_m)/I_0^2(\tau_m)\right)/a_2^2\tau_m^2 + \left(1-I_0^2(\tau_m)/I_1^2(\tau_m)\right)\tan^2\psi - (1+\tilde{\tau}_m^{-2}\Delta_{m11}^{-2}(1)\\ &\quad -\Delta_{m10}^2(1)/\Delta_{m11}^2(1))\tan^2\psi - \varepsilon_{\mathit{eff}}^2\left(1+\tilde{\tau}_m^2\Delta_{m00}^{-2}(1)-\Delta_{m01}^2(1)/\Delta_{m00}^2(1)\right)/a_2^2\tilde{\tau}_m^2\end{aligned}$$

and $\mathrm{sgn}(n)$ denotes the sign of n. Once the arbitrary constants $\bar{A}_{mn}(n = \pm\beta_m/k_d)$ appearing in the solution (B3) for $E_{kmn}(r)$ and $H_{kmn}(r)$, $k = 1, 2, 3$ have been uniquely determined according to (B6), we may set $A_{mn} \equiv 0$ ($n = \pm\beta_m/k_d$) without any loss in generality as nonzero values of A_{mn} may be absorbed in the arbitrary constants $A_m^{\pm}$ appearing in the homogeneous part of the solution.

When there is resonance, that is, when the set Q is nonempty, the expression (41) for the axial electric field component gets modified to

$$\begin{aligned}\boldsymbol{\mathcal{E}}_1(z,r,t) = {} & \delta_{1m}W_1(r)\left((A/2)\exp(j(t-\beta_1 z)) + c.c.\right) + (jq_0/2\pi a_1 d) \\ & \sum_{\substack{m=1 \\ m\notin Q}}^{\infty}(1/m)\exp(jmt)\int_0^d dx\int_0^a G_m(z,r;x,y)ydy\int_{-\pi}^{\pi}\exp\{-jmt(x,y,\tau)\}d\tau + c.c. + (jq_0/\pi a_1 d) \\ & \sum_{m\in Q}(1/m)\exp(jmt)\int_0^d dx\int_0^a \bar{G}_m(z,r;x,y)ydy\int_{-\pi}^{\pi}\exp\{-jt(x,y,\tau)\}d\tau + c.c. \end{aligned} \tag{B7}$$

where

$$\begin{aligned}\bar{G}_m(z,r;x,y) = {} & \left[\left(\bar{G}_{mn}(r,y) - W_m(r)\bar{G}_{mn}(1,y)\right)\cos\beta_m z \right. \\ & \left. -\left(zW_m(r)I_0(\tau_m y)\sin\beta_m z/\beta_m\Delta_m I_0(\tau_m)\right)\right]\cos\beta_m x \end{aligned} \tag{B8}$$

and where

$$\bar{G}_m(r,y) = \begin{cases} rI_1(\tau_m r)I_1(\tau_m y)/\tau_m\Delta_m I_0^2(\tau_m) - \tau_m^2\tilde{G}_m(r,y)1_{[0,r\wedge a]}(y) & \text{for } 0\le r<1 \text{ and } 0\le y\le a \\ \left[I_1(\tau_m)\Delta_{m00}(r)/a_2^2\Delta_m\tau_m I_0^2(\tau_m)\Delta_{m00}(1) + \left(\varepsilon_{\mathit{eff}}/\tilde{\tau}_m\Delta_{m00}^2(1)I_0(\tau_m)\right)\right. & \\ \left.\{\Delta_{m01}(1)\Delta_{m00}(r) - r\Delta_{m00}(1)\Delta_{m01}(r) + bK_0(\tilde{\tau}_m)I_0(\tilde{\tau}_m r) - bI_0(\tilde{\tau}_m)K_0(\tilde{\tau}_m r)\}\right] & \\ I_0(\tau_m y) - \tau_m^2(\Delta_{m00}(r)\Delta_{m00}(1))\tilde{G}_m(1,y) & \text{for } 1<r<b \text{ and } 0\le y\le a \end{cases} \tag{B9}$$

In numerical computations, in order to avoid the problem of small divisors, it is expedient to take $\varepsilon_{mn} = 1$ in (B2), even when $|n|k_d$ is very close to, but not coincident with β_m.

REFERENCES

1. Pierce, J. R. and L. M. Field, "Traveling wave tubes," *Proc. IRE*, Vol. 35, 108–111, 1947.
2. Pierce, J. R., "Theory of the beam-type traveling wave tube," *Proc. IRE*, Vol. 35, 111–123, 1947.
3. Kompfner, R., "The traveling wave tube as amplifier at microwaves," *Proc. IRE*, Vol. 35, 124–128, 1947.
4. Rydbeck, O. E. H., "Theory of the traveling wave tubes," *Ericsson Technics*, Vol. 46, 03-18, 1948.
5. Chu, L. J. and J. D. Jackson, "Field theory of traveling wave tubes," *Proc. IRE*, Vol. 36, 853–863, 1948.
6. Collin, R. E., *Foundations for Microwave Engineering*, 2nd edition, IEEE Press, 2005.
7. Rowe, J. E., *Nonlinear Electron-wave Interaction Phenomena*, Academic Press, 1965.
8. Freund, H. P., M. A. Kodis, and N. R. Vanderplaats, "Design of traveling wave tubes based on field theory," *IEEE Trans. on Electron Devices*, Vol. 41, No. 7, 1288–1296, 1994.
9. Freund, H. P., E. G. Zaidman, M. A. Kodis, and N. R. Vanderplaats, "Linearized field theory of a dielectric-loaded helix traveling wave tube amplifier," *IEEE Trans. on Plasma Science*, Vol. 24, No. 3, 895–904, 1996.
10. Detweiler, H. K. and J. E. Rowe, "Electron dynamics and energy conversion in O-type linear beam devices," *Advances in Microwaves*, Young, L., Ed., Vol. 6, 29–123, Academic Press, 1971.
11. Kalyanasundaram, N., "Large signal field analysis of an O-type traveling wave amplifier. Part 1: Theory," *IEE Proc. I, Solid-State* & *Electron Dev.*, Vol. 131, No. 5, 145–152, 1984.
12. Kalyanasundaram, N. and R. Chinnadurai, "Large signal field analysis of an O-type traveling wave amplifier. Part 2: Numerical results," *IEE Proc. I, Solid-State* & *Electron Dev.*, Vol. 133, No. 4, 163–168, 1986.

13. Kalyanasundaram, N. and R. Chinnadurai, "Large signal field analysis of an O-type traveling wave amplifier. Part 3: Three-dimensional electron motion," *IEE Proc. I, Solid-State* & *Electron Dev.*, Vol. 135, No. 3, 59–66, 1988.
14. Jain, P. K. and B. N. Basu, "The Inhomogeneous loading effects of practical dielectric supports for the helical slow-wave structure of a TWT," *IEEE Trans. on Electron Devices*, Vol. 34, No. 12, 2643–2648, 1987.
15. Gewartowski, J. W. and H. A. Watson, *Principles of Electron Tubes*, Van Nostrand, 1968.
16. Naylor A. W. and G. R. Sell, *Linear Operator Theory in Engineering and Science*, Springer-Verlag, 1982.
17. Agnihotri, A., "Large-signal field analysis of a linear beam traveling wave amplifier for a dielectric-loaded sheath helix model of the slow-wave structure," Forthcoming Ph.D. Dissertation, Jaypee Institute of Information Technology, Noida, India, 2014.
18. Thomas, J. B., *Introduction to Probability*, Springer-Verlag, 1986.
19. Jacod, J. and P. Protter, *Probability Essentials*, 2nd edition, Springer, 2003.
20. Kalyanasundaram, N. and G. N. Babu, "Propagation of electromagnetic waves guided by anisotropically conducting model of a tape helix supported by dielectric rods," *Progress In Electromagnetics Research B*, Vol. 51, 81–99, 2013.